

Electronic Supplementary Information

# Environmental impacts of III-V / silicon photovoltaics: life cycle assessment and guidance for sustainable manufacturing

Carlos Felipe Blanco<sup>a,\*</sup>, Stefano Cucurachi<sup>a</sup>, Frank Dimroth<sup>b</sup>, Willie J.G.M. Peijnenburg<sup>a,c</sup>, Jeroen B. Guinée<sup>a</sup>, Martina G. Vijver<sup>a</sup>

<sup>a</sup> Institute of Environmental Sciences (CML), Leiden University, Leiden, The Netherlands

<sup>b</sup> Fraunhofer Institute for Solar Energy Systems, Heidenhofstr. 2, 79110 Freiburg, Germany

<sup>c</sup> National Institute of Public Health and the Environment (RIVM), Center for Safety of Substances and Products, Bilthoven, The Netherlands

## Contents

1.	System flowcharts and boundaries .....	2
2.	Life-cycle inventories: process descriptions and input/output data.....	4
2.1.	Overview and general assumptions .....	4
2.2.	Silicon wafer preparation .....	4
2.3.	Ion implantation (p-n junction) .....	4
2.4.	Tube furnace annealing – high temperature.....	4
2.5.	Atomic layer deposition (ALD).....	5
2.6.	Back-side passivation.....	5
2.7.	III-V Metalorganic Vapor Phase Epitaxy (MOVPE).....	5
2.8.	Front metal contacts .....	6
2.8.1.	Seed layer (nano) inkjet printing .....	6
2.8.2.	Seed layer sintering: laser .....	6
2.8.3.	Seed layer sintering: chemical (Cu ink only).....	7
2.8.4.	Fingers electroplating.....	7
2.8.5.	Busbars screen printing.....	8
2.9.	Rear-side metal contacts .....	8
2.10.	Tube furnace annealing - low temperature .....	8
2.11.	Carrier gases .....	9
2.11.1.	Ultrapure hydrogen .....	9
2.11.2.	Ultrapure nitrogen.....	10
2.12.	Hydride gases .....	10
2.13.	Metalorganic precursors .....	10
2.14.	Scrubbing of MOVPE and ion implant exhaust gas .....	11
2.15.	III-V MOVPE growth on GaAs substrate .....	11
2.16.	Bonding.....	12
2.17.	Lift-off .....	13
2.17.1.	Laser lift-off .....	13
2.17.2.	Chemical lift-off .....	13
2.18.	GaAs substrate reuse and reclaim.....	13
2.19.	III-V/Si PV electricity generation.....	14
	References.....	16

## 1. System flowcharts and boundaries

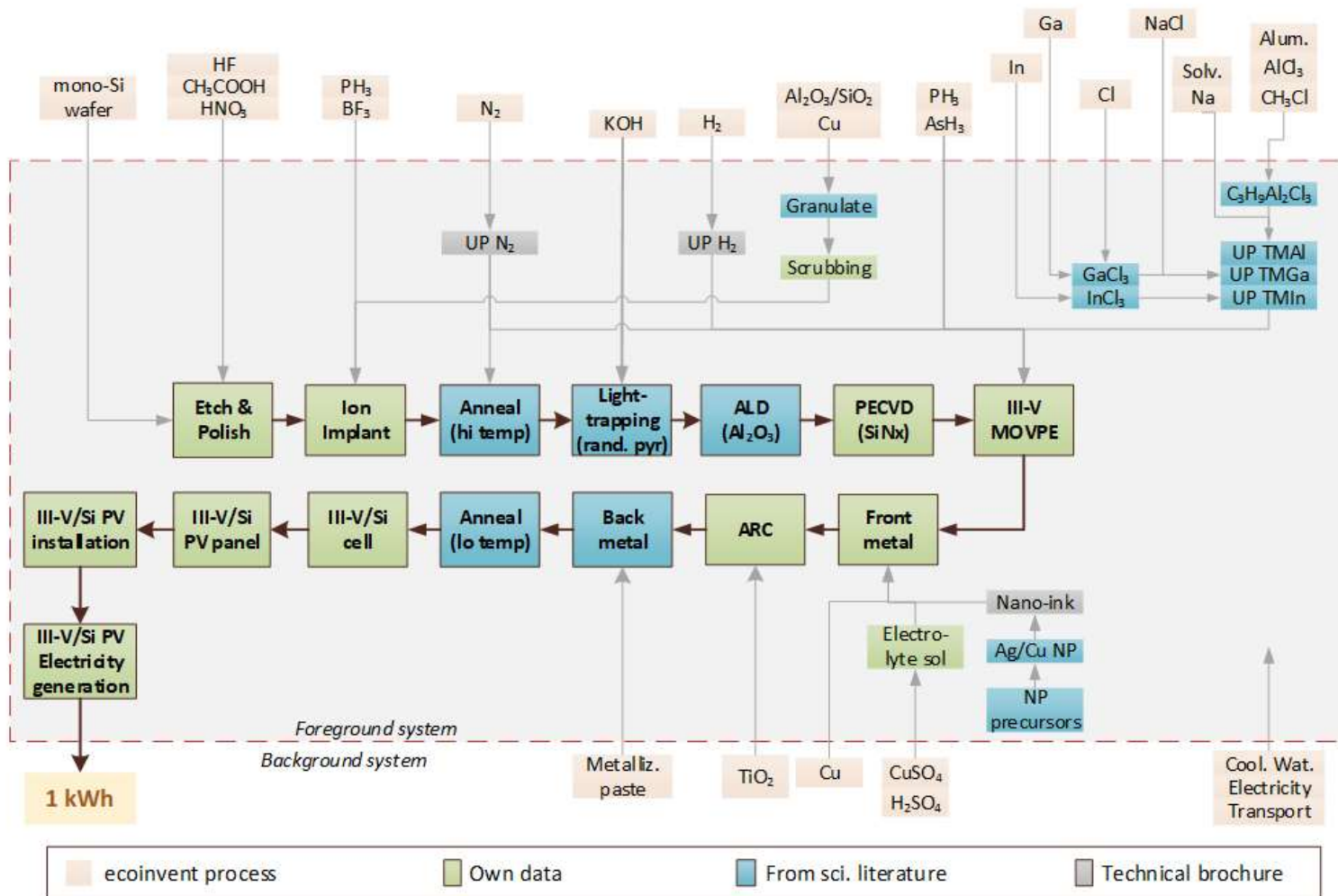


Figure S1 Product system flowchart for Concept A (direct growth). UP = Ultrapure.

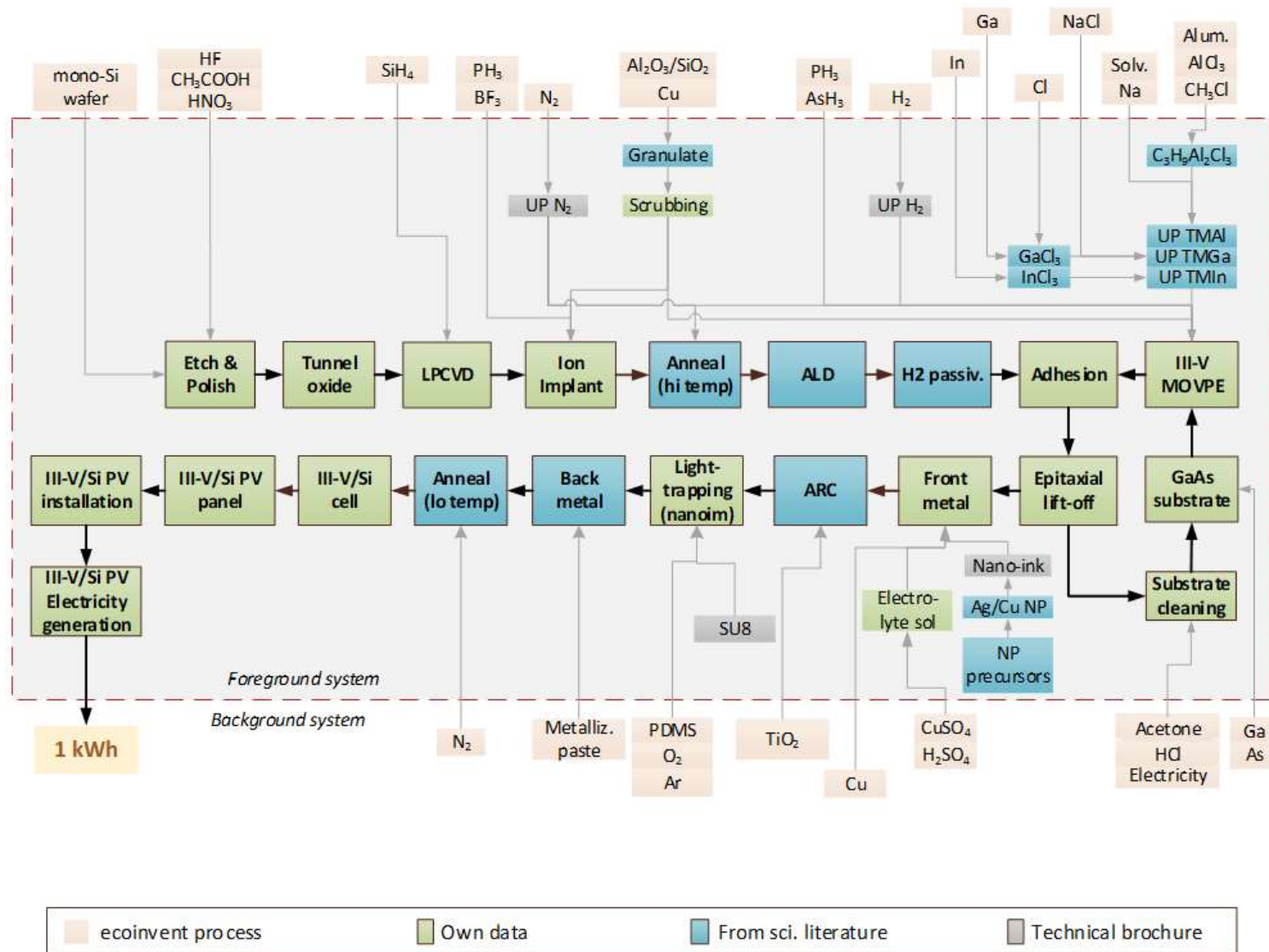


Figure S2 Product system flowchart for Concept B (bonding). UP = Ultrapure.

## 2. Life-cycle inventories: process descriptions and input/output data

### 2.1. Overview and general assumptions

Most of the foreground processes are sensitive to the wafer area that can be processed per run, since materials and energy consumption scale proportionally with the treatable wafer area. We based our models on the use of a large MOVPE reactor prototype designed by AIXTRON, which can handle a run of 31 4-inch wafers with a total area of 2,905 cm<sup>2</sup>. We assumed that all other processing steps would handle wafers of the same area.

We also note here that some lab-based processes described below have been modelled considering only process inputs, while waste emissions have not been fully characterized. The characterization of waste streams and emissions is more relevant in industrial-scale implementations where recycling and reuse take a central role and differ significantly from waste management in a lab environment. However, based on extrapolation from similar processes, it appears that these emissions would only have relatively minor contributions to the life cycle impacts of the electricity generation process.

### 2.2. Silicon wafer preparation

Table S1. Process inputs and outputs for silicon wafer preparation

Input	Flow type	Quantity	Data source
CZ single-Si wafer	Eco	100 units	TopSil, personal communication
HF	Eco	0.3 L	TopSil, personal communication
HNO <sub>3</sub>	Eco	1.6 L	TopSil, personal communication
HC <sub>2</sub> H <sub>2</sub> O <sub>2</sub>	Eco	0.1 L	TopSil, personal communication
Treatment of wastewater from PV cell production	Eco	2 L	TopSil, personal communication
Output	Flow type	Quantity	Data source
Polished Si wafer	Eco	100 units	TopSil, personal communication

### 2.3. Ion implantation (p-n junction)

Table S2. Process inputs and outputs for ion implantation

Input	Flow type	Quantity	Data source
Phosphine (PH <sub>3</sub> )	Eco	3.4 g	Fraunhofer, personal communication
Boron trifluoride (BF <sub>3</sub> )	Eco	3.4 g	Fraunhofer, personal communication
Ultrapure nitrogen (N <sub>2</sub> )	Eco	14 m <sup>3</sup>	Fraunhofer, personal communication
Cooling water	Eco	5 m <sup>3</sup>	Fraunhofer, personal communication
Electricity, high voltage	Eco	100 kWh	Fraunhofer, personal communication
Compressed air	Eco	15 m <sup>3</sup>	Fraunhofer, personal communication
Hazardous waste incineration	Eco	0.009 kg	Calculated
Output	Flow type	Quantity	Data source
Doped wafer area (3400 wafers)	Eco	26.69 m <sup>2</sup>	Fraunhofer, personal communication

### 2.4. Tube furnace annealing – high temperature

We assumed the use of a 4.2kW power furnace which can handle 100 wafers per batch. The wafers cannot be inserted at 1000°C; this has to be done at <400°C, and then the temperature is ramped up at a rate of 10°C per minute. The annealing time is 1 hour at 1000°C and the temperature is then

ramped down for removal of the wafers. We assume a worst case scenario where the furnace operates at full power during ramp up and processing time. We assume no power is consumed during ramp-down. Annealing is conducted in an inert environment of ultrapure nitrogen, which flows at a rate of 30 SLM (standard litres per minute) during insertion and removal, and 15 SLM during annealing.

Table S3. Process inputs and outputs for high temperature tube furnace annealing

Flow type	Flow type	Quantity	Data source
Ultrapure nitrogen	Eco	0.9 m <sup>3</sup>	AZUR, personal communication
Electricity	Eco	10.668 kWh	Calculated
Output	Flow type	Quantity	Data source
Annealing of 1 m <sup>2</sup> of cell	Eco	1 unit	Calculated

## 2.5. Atomic layer deposition (ALD)

This step considers the deposition of a 10nm film of Al<sub>2</sub>O<sub>3</sub> on the rear side. Process data for this step is based on Louwen et al.<sup>1</sup>, who reviewed various specifications and found average electricity use to be 0.29 kWh/m<sup>2</sup>, with values ranging 0.15 to 0.51 kWh/m<sup>2</sup> (-48% to +76%). No materials input data and output data was available for this step.

## 2.6. Back-side passivation

Back-side passivation is conducted by plasma-enhanced chemical vapour deposition (PECVD) of a SiNx layer.

Table S4. Energy and material inputs and outputs for PECVD back-side passivation

Input	Flow type	Quantity	Data source
Electricity	Eco	39,93 Wh	Fraunhofer, personal communication
Cooling water	Eco	5,27 L	Fraunhofer, personal communication
Nitrogen	Eco	12,57 L	Fraunhofer, personal communication
Compressed dry air	Eco	5,02 L	Fraunhofer, personal communication
Silane (SiH <sub>4</sub> )	Eco	0,03 L	Fraunhofer, personal communication
NH <sub>3</sub>	Eco	0,06 L	Fraunhofer, personal communication
Output	Flow type	Quantity	Data source
Back-side passivation of 1 cell	Eco	1 unit	Fraunhofer, personal communication

## 2.7. III-V Metalorganic Vapor Phase Epitaxy (MOVPE)

Table S5. Process inputs and outputs for MOVPE III-V direct growth

Flow type	Flow type	Quantity	Data source
TMGa	Eco	11.48 g	Aixtron, personal communication
TMIIn	Eco	0.1 g	Aixtron, personal communication
TMAI	Eco	0.17 g	Aixtron, personal communication
AsH <sub>3</sub>	Eco	11.76 g	Aixtron, personal communication
PH <sub>3</sub>	Eco	17.84 g	Aixtron, personal communication
H <sub>2</sub>	Eco	3.34 m <sup>3</sup>	Aixtron, personal communication
N <sub>2</sub>	Eco	3.44 m <sup>3</sup>	Aixtron, personal communication
Cooling water	Eco	27.51 m <sup>3</sup>	Aixtron, personal communication

<b>Electricity</b>	Eco	105.06 kWh	Aixtron, personal communication
<b>Hazardous waste treatment</b>	Eco	0.035 kg	Calculated
<b>Output</b>	Flow type	Quantity	Data source
<b>III-V layer area</b>	Eco	2905 cm <sup>2</sup>	Aixtron, personal communication

## 2.8. Front metal contacts

We based our model on a “seed and plate” metallization technique, which involves nanoink printing of a seed layer of fingers, then electroplating to increase the thickness of the fingers. Conventional screen-printing methods are considered for 3 busbars that cross the fingers.

### 2.8.1. Seed layer (nano) inkjet printing

**Materials:** The pattern to be printed on the cells for the seed layer consists of 6 fingers 2 mm wide, 75 mm long and 0.1 μm thick (height) on average. The total quantity of nanoink required is calculated by the total volume of this pattern multiplied by the density of the nanoink (reported by the manufacturer). To this quantity, we added 10% to account for ink that remains in the filter and is discarded as hazardous waste. Therefore, we have the following inputs, per cell:

$$\begin{array}{cccccc} \# \text{ fingers} & \text{Finger width} & \text{Finger length} & \text{Finger thickness} & \text{Ink density} & \text{Loss factor} \\ 6 \cdot \left( 2 \text{ mm} \cdot \frac{1 \text{ m}}{1E3 \text{ mm}} \right) \cdot \left( 75 \text{ mm} \cdot \frac{1 \text{ m}}{1E3 \text{ mm}} \right) \cdot \left( 0.1 \mu\text{m} \cdot \frac{1 \text{ m}}{1E6 \mu\text{m}} \right) \cdot \frac{1.27E3 \text{ kg}}{\text{m}^3} \cdot 110\% = 1.25E-7 \text{ kg Cu ink} \end{array}$$

**Printer electricity.** A sample tested at Joanneum Research Center facilities was approximately 10 cm. long and took 5 minutes to print, with only 2 nozzles in use out of a total possible of 210. We estimated the printing speed as:

$$\frac{10 \text{ cm}}{5 \text{ min}} \cdot \frac{210 \text{ nozzles}}{2 \text{ nozzles}} \cdot \frac{60 \text{ min}}{1 \text{ h}} \cdot \frac{1 \text{ m}}{100 \text{ cm}} = \frac{126 \text{ m}}{\text{h}}$$

From the data in section 1.1, the total length of the 6 printed fingers is 0.45 m, and the printer has a maximum power rating of 1kW. We assume it operates at 75% power on average. To calculate electricity consumption of the printing process (per cell) we have:

$$\frac{0.45 \text{ m}}{\text{cell}} \cdot \frac{1 \text{ h}}{126 \text{ m}} \cdot 1 \text{ kW} \cdot 75\% = \frac{0.027 \text{ kWh}}{\text{cell}}$$

### 2.8.2. Seed layer sintering: laser

**Laser electricity:** The length of the pattern that has to be sintered is calculated from the data in the previous section (0.45 m). We used a laser scan speed of 0.01 m/s, and the optical power delivered by the laser is 1.4 W. The wall-plug to optical efficiency of YAG type lasers is typically around 25%<sup>2</sup>, so we estimate the electricity consumption for laser sintering as:

$$\frac{0.45 \text{ m}}{\text{cell}} \cdot \frac{\text{s}}{0.01 \text{ m}} \cdot \frac{1 \text{ h}}{3600 \text{ s}} \cdot 1.4E-3 \text{ kW} \cdot \frac{1}{25\%} = \frac{5.6E-5 \text{ kWh}}{\text{cell}}$$

**Materials:** Laser-sintering of both Cu and Ag ink is done in open air.

Table S6. Process inputs and outputs for seed-layer inkjet printing

Flow type	Flow type	Quantity	Data source
Cu nanoink	Eco	1.25E-7 kg	Joanneum, personal communication
Electricity	Eco	0.0271 kWh	Joanneum, personal communication
Output	Flow type	Quantity	Data source
Finger seed layers for 1 cell	Eco	1 unit	Joanneum, personal communication

### 2.8.3. Seed layer sintering: chemical (Cu ink only)

Sintering of Cu ink requires a reducing environment, while Ag ink can be sintered in open air. For the Cu ink, a sintering test was conducted at Joanneum Research Center facilities, where for a 1cm<sup>2</sup> sample 5 mL of ethanol (3.95 g @ 789g/L), 50 mL formic acid, and 70 L of ultrapure nitrogen were required.

### 2.8.4. Fingers electroplating

Electroplating consists of submerging the cell with the seed pattern in an electrolyte bath, where the patterned cell will serve as an ion-receiving cathode and a copper in the solution will serve as an anode. For copper, the electrolyte solution consists of a mix of cupric sulphate and sulphuric acid. Driving an electric current through the solution will force the metallic ions from the cathode to deposit on the seed pattern until the desired geometry is obtained.

Electricity: A conventional electroplating setup is used, where 10 mA of applied current with an average voltage of 0.5 V provides 250 nm of plating per minute. The electrical power can be calculated from the current and voltage:

$$P = I \cdot V = \left(10 \text{ mA} \cdot \frac{1 \text{ A}}{1000 \text{ mA}}\right) \cdot (0.5 \text{ V}) = 5 \text{ E} - 3 \text{ W} = 5 \text{ E} - 6 \text{ kW}$$

The amount of electricity consumed is calculated by multiplying the power by the time required to plate the desired finger thickness of 12.5µm.

$$\frac{5 \text{ E} - 6 \text{ kW}}{\text{cells}} \cdot \frac{1 \text{ min}}{0.25 \text{ } \mu\text{m}} \cdot 12.5 \text{ } \mu\text{m} \cdot \frac{1 \text{ h}}{60 \text{ min}} = \frac{4.16 \text{ E} - 6 \text{ kWh}}{\text{cell}}$$

Materials: Pure metal anodes donate the ions that ultimately deposit on the pattern (cathode). The ions are first passed from the electrolyte solution to the cathode, and are then replenished from the anode to the solution. Therefore, the anode is sacrificed according to the amount of metal deposited in the cell, and we assume 10% losses.

$$\text{Cu: } 6 \cdot \left(2 \text{ mm} \cdot \frac{1 \text{ m}}{1 \text{ E}3 \text{ mm}}\right) \cdot \left(75 \text{ mm} \cdot \frac{1 \text{ m}}{1 \text{ E}3 \text{ mm}}\right) \cdot \left(12.4 \text{ } \mu\text{m} \cdot \frac{1 \text{ m}}{1 \text{ E}6 \text{ } \mu\text{m}}\right) \cdot \frac{8.96 \text{ E}3 \text{ kg}}{\text{m}^3} \cdot 110\% = 1.09 \text{ E} - 4 \text{ kg Cu}$$

We consider a standard cupric sulphate electrolyte solution that consists of 200 g cupric sulphate and 25 mL sulphuric acid in sufficient deionized water to prepare 1 L of electrolyte solution. This amount of solution is used for electroplating on one cell; however, we consider that it can be used for the production of 10-100 wafers based on lab experience, and test the sensitivity of this parameter.

Table S7. Energy and material inputs and outputs for electroplating of fingers

Flow type	Flow type	Quantity	Data source
Copper	Eco	1.09E-4 kg	Joanneum, personal communication
Electricity	Eco	4.16E-6 kWh	Joanneum, personal communication
Electrolyte solution	Eco	0.1 L	Joanneum, personal communication
Output	Flow type	Quantity	Data source
Electroplating of 1 cell	Eco	1 unit	Joanneum, personal communication

### 2.8.5. Busbars screen printing

Screen printing electricity: We use data from a screen printer running a squeegee motor with a power of 1.16 kW. The printer can process a sheet of 400x400mm in 30 seconds.

$$\frac{1 \text{ sheet}}{4 \text{ cells}} \cdot 1.16 \text{ kW} \cdot 30 \text{ s} \cdot \frac{1 \text{ h}}{3600 \text{ s}} = \frac{2.41E-3 \text{ kWh}}{\text{cell}}$$

Curating electricity: Cu busbars are grown over the Cu fingers by screen-printing. However, instead of co-firing, the Cu busbars are curated at lower temperature (250°C) in an atmosphere of pure nitrogen<sup>3</sup>. This is done in a furnace that has a power rating of 3.4 kW and can process 1000 cells per batch, for a curating time of 10 minutes.

$$\frac{3.4 \text{ kW}}{1000 \text{ cells}} \cdot 10 \text{ min} \cdot \frac{1 \text{ h}}{60 \text{ min}} = \frac{5.67E-4 \text{ kWh}}{\text{cell}}$$

Materials: We consider 3 busbars, 1 mm wide, 156 mm long and 13.5 µm thick on average. We assume 10% losses from the paste during screen-printing. Per cell, we have:

$$3 \cdot \left(1 \text{ mm} \cdot \frac{1 \text{ m}}{1E3 \text{ mm}}\right) \cdot \left(156 \text{ mm} \cdot \frac{1 \text{ m}}{1E3 \text{ mm}}\right) \cdot \left(13.5 \text{ } \mu\text{m} \cdot \frac{1 \text{ m}}{1E6 \text{ } \mu\text{m}}\right) \cdot \frac{8.96E3 \text{ kg}}{\text{m}^3} \cdot 110\% = 6.23E-5 \text{ kg Cu}$$

Table S8. Energy and material inputs and outputs for screen printing of busbars

Flow type	Flow type	Quantity	Data source
Copper	Eco	6.23E-5 kg	Joanneum, personal communication
Electricity	Eco	3E-3 kWh	Joanneum, personal communication
Output	Flow type	Quantity	Data source
Screen printing of 1 cell	Eco	1 unit	Joanneum, personal communication

### 2.9. Rear-side metal contacts

Data for the rear-side metal contacts are taken from the inventories for existing single-Si PV cells (ecoinvent v3.4)<sup>4</sup>.

### 2.10. Tube furnace annealing - low temperature

The data for this process was calculated as for the high temperature annealing in section 2.4; however we discard ramp up energy and gas flow requirements, since the cells can be inserted and removed at this lower process temperature (<400°C).

## 2.11. Carrier gases

### 2.11.1. Ultrapure hydrogen

Two alternatives are considered for the supply of ultrahigh purity hydrogen: off-site source (commercially available hydrogen produced from Steam Methane Reforming) and on-site generation with a proton exchange membrane (PEM) system. In both alternatives, additional purification with a two-step adsorber/getter is considered.

*Off-site generation: Commercial H<sub>2</sub> gas + adsorber/getter.* Commercial production of hydrogen gas is modelled based on the steam methane reforming process (SMR), which accounts for over 90% of the world production. This production method was modelled in an LCA study by NREL<sup>5</sup> and more recently by other authors<sup>6,7</sup>. We use the process data reported by Cetinkaya et al.<sup>7</sup>, which is in close accordance with figures reported by Mehmeti et al.<sup>6</sup> The inputs required for generating electricity that is consumed in the SMR process are also included in the inventory.

Table S9. Process inputs and outputs for production of hydrogen via steam methane reforming

Input	Flow type	Quantity	Data source
Concrete	Eco	5.26E-06 m <sup>3</sup>	Cetinkaya et al. <sup>7</sup>
cast iron	Eco	0.049 g	
steel, low-alloyed	Eco	4.029 g	
aluminium, cast alloy	Eco	0.033 g	
water, deionised	Eco	19,776.2 g	
natural gas; 44.1 MJ/kg	Env	165 MJ	
Coal, hard, unspecified, in ground	Env	132.49 g	
Oil, crude, in ground	Env	8.76 g	
Output	Flow type	Quantity	Data source
Hydrogen	Eco	1 kg	Cetinkaya et al. <sup>7</sup>

The purifier (adsorber + getter) commercialized by SAES Gas handles a flow of 100 Nm<sup>3</sup>/h at an average power consumption of 26kW, therefore 0.26kWh/Nm<sup>3</sup>. It also consumes 60 L/min of cooling water, therefore 0.036 m<sup>3</sup> water/Nm<sup>3</sup>. In this case we include transportation from SMR plant to consumer, using the same values as for liquid hydrogen specified in EcoInvent v3.4.

Table 3. Process inputs and outputs for purification of hydrogen

Input	Flow type	Quantity	Data source
Hydrogen	Eco	0.08988 kg	SAES product spec sheet
Electricity	Eco	0.26 kWh	SAES product spec sheet
Cooling water	Eco	0.036 m <sup>3</sup>	SAES product spec sheet
transport, freight train	Eco	0.0004 t*km	EcoInvent v3.4
transport, freight, light commercial vehicle	Eco	1.62E-05 t*km	EcoInvent v3.4
transport, freight, lorry, unspecified	Eco	0.00051 t*km	EcoInvent v3.4
Output	Flow type	Quantity	Data source
Ultrapure hydrogen	Eco	1 Nm <sup>3</sup>	SAES / Proton product spec sheets

*On-site generation: PEM on-site generator + adsorber/getter.* The proton exchange membrane (PEM) generator commercialized by Proton delivers 30 Nm<sup>3</sup>/hr, consuming 5.8 kWh / Nm<sup>3</sup> on average. (For consistency check, we compare with Mehmeti et al.<sup>6</sup> who separately report a consumption of 54.6 kWh/kgH<sub>2</sub> = 4.5 kWh/Nm<sup>3</sup>. Balahi et al.<sup>8</sup> report a consumption of 4.775 kWh/Nm<sup>3</sup>). The Proton PEM generator also requires 26.9 L/h of deionized water per hour and 167 L/min coolant. The purifier (adsorber + getter) commercialized by SAES Gas handles a flow of 100 Nm<sup>3</sup>/h at an average power consumption of 26kW, therefore 0.26kWh/Nm<sup>3</sup>. It also consumes 60 L/min of cooling water, therefore 0.036 m<sup>3</sup> water/Nm<sup>3</sup>. Data for the combined processes is presented in Table S11.

Table S11. Process inputs and outputs for onsite generation and purification of hydrogen

Input	Flow type	Quantity	Data source
Electricity	Eco	6.022 kWh	SAES / Proton product spec sheets
DI water	Eco	0.897 kg	Proton product spec sheet
Cooling water	Eco	0.34 m <sup>3</sup>	SAES product spec sheet
Output	Flow type	Quantity	Data source
Ultrapure hydrogen	Eco	1 Nm <sup>3</sup>	SAES / Proton product spec sheets

### 2.11.2. Ultrapure nitrogen

We consider the use of commercially available liquid nitrogen, which is produced via cryogenic air separation and delivered to consumers in the European market as per EcoInvent v3.4.<sup>4</sup> Although the nitrogen produced via this method is of high purity (99.9999%), we consider additional purification on-site using data for a commercially available SAES purifier.

Table S12. Process inputs and outputs for purification of nitrogen for MOVPE application

Input	Flow type	Quantity	Data source
Nitrogen	Eco	1.25 kg	EcoInvent v3.4
Electricity	Eco	3.3E-4 kWh	SAES product spec sheet
Cooling water	Eco	6.4E-4 m <sup>3</sup>	
Output	Flow type	Quantity	Data source
Ultrapure nitrogen	Eco	1 Nm <sup>3</sup>	SAES product spec sheets

### 2.12. Hydride gases

Hydride gases arsine and phosphine were taken directly from the EcoInvent v3.4 database.<sup>4</sup> It is known that further purification may be required to reduce acids and humidity that result from cylinder use, and this can be achieved by commercially available purifiers that use an adsorbent medium. However, no specific data for this purification process was available at the time of this report. It is flagged, however, as an important follow-up area due to the potential generation of significant amounts of hazardous waste in the form of adsorbent media.

### 2.13. Metalorganic precursors

We used the input/output data for the synthesis of metalorganic precursors for III-V MOVPE reported by Smith et al. (2018)<sup>9</sup>.

## 2.14. Scrubbing of MOVPE and ion implant exhaust gas

We assumed dry scrubbing systems, in which the main component is an adsorbent granulate. Energy is only required to operate the equipment systems and monitors, but not for the reaction, therefore it was assumed negligible. Based on tests run at Fraunhofer ISE facilities, 17 kg of hydride gases (arsine or phosphine) from an MOVPE reactor were absorbed in 130 kg of granulate.

Granulate composition is not disclosed by manufacturers, but a review of literature, patents, safety data sheets and technical brochures indicates that the industry is moving towards chemisorption by copper oxide catalyst impregnated on a supporting medium of alumina ( $\text{Al}_2\text{O}_3$ ) or silicate ( $\text{SiO}_2$ )<sup>10-13</sup>. Another option is the use of zeolite (a microporous aluminosilicate mineral) exchanged with a copper cation. After adsorption, the granulate is collected and reprocessed externally into new copper for other industrial uses. No information could be found on intermediate processing steps.

For the zeolite based adsorbent, we modelled the process described Wang and colleagues<sup>14</sup> for the adsorption of arsine, which is similar to the process described by Li and colleagues<sup>15</sup> for phosphine. We chose the best performing alternative presented by the authors, a copper-loaded zeolite, which is produced by impregnating the zeolite in a 50 mL solution of copper II nitrate with a concentration of 0.2 mol/L  $\text{Cu}(\text{NO}_3)_2$ . Based on the preparation procedure reported by the authors, the inputs and outputs are:

Table S13. Process inputs and outputs for purification of scrubbing of arsine and phosphine

Input	Flow type	Quantity	Data source
<b>Zeolite adsorbent</b>	Eco	7.65 kg	Fraunhofer, personal communication
<b>Hazardous waste, for underground deposit</b>	Eco	-8.65 kg	Calculated as mass of adsorbent + mass of treated gas.
Output	Flow type	Quantity	Data source
<b>III-V waste gas treatment</b>	Eco	-1 kg	Fraunhofer, personal communication

Table S14. Process inputs and outputs for production of copper zeolite adsorbent granulate

Input	Flow type	Quantity	Data source
<b>Zeolite powder</b>	Eco	10 g	Wang et al. <sup>14</sup>
<b>Copper II nitrate</b>	Eco	2.95 g	Wang et al. <sup>14</sup> . Based on molar mass of $\text{Cu}(\text{NO}_3)_2$ . Authors report 10% Cu(II) content by weight in final adsorbent. Starting mass of zeolite is 10 g
Output	Flow type	Quantity	Data source
<b>Zeolite adsorbent</b>	Eco	12.95 g	Wang et al. <sup>14</sup> .

## 2.15. III-V MOVPE growth on GaAs substrate

Table S15. Process inputs and outputs for MOVPE III-V growth on GaAs substrate

Flow type	Flow type	Quantity	Data source
<b>TMGa</b>	Eco	5.26 g	Aixtron, personal communication
<b>TMIIn</b>	Eco	1.23 g	Aixtron, personal communication
<b>TMAI</b>	Eco	3.17 g	Aixtron, personal communication

AsH3	Eco	19.96 g	Aixtron, personal communication
PH3	Eco	4.15 g	Aixtron, personal communication
H2	Eco	0.93 m3	Aixtron, personal communication
N2	Eco	2.24 m3	Aixtron, personal communication
Cooling water	Eco	17.89 m3	Aixtron, personal communication
Electricity	Eco	68.33 kWh	Aixtron, personal communication
Hazardous waste treatment	Eco	0.024 kg	Calculated
<b>Output</b>	<b>Flow type</b>	<b>Quantity</b>	<b>Data source</b>
III-V layer area	Eco	2905 cm <sup>2</sup>	Aixtron, personal communication

## 2.16. Bonding

The bonding process as described by Heitmann et al.<sup>16</sup> requires 4 steps: HF clean, spray pyrolysis, adhesion and hot press. For the hot-press we used parameters from a commercial wafer bonding tool (<https://www.suss.com/en/products-solutions/wafer-bonder/sb6-sb8-gen2>). The tool has a power rating of 4.2kW and can process up to 8 wafers simultaneously. We assumed a bonding time of 20 minutes.

Table S16. Process inputs and outputs for bonding

Input	Flow type	Quantity	Data source
HF	Eco	3.44 g	Fraunhofer ISE, personal communication
Spray pyrolysis solution	Eco	120 mL	Fraunhofer ISE, personal communication
Electricity	Eco	0.175 kWh	Fraunhofer ISE, personal communication
<b>Output</b>	<b>Flow type</b>	<b>Quantity</b>	<b>Data source</b>
Bonding of 1 III-V/Si cell	Eco	1 unit	

Table S17. Process inputs and outputs for bonding of spray pyrolysis solution.

Input	Flow type	Quantity	Data source
Zinc 2,4 pentanedione	Eco	1.7 g	Fraunhofer ISE, personal communication
Methanol	Eco	20.0 g	Fraunhofer ISE, personal communication
Indium trichloride	Eco	1.32 g	Fraunhofer ISE, personal communication
<b>Output</b>	<b>Flow type</b>	<b>Quantity</b>	<b>Data source</b>
Spray pyrolysis solution	Eco	1 L	

There are several routes for the industrial synthesis of zinc 2,4 pentanedione (which is a metal acetylacetonate)<sup>17</sup>; we consider a reaction of the zinc chloride salt with acetylacetone and use stoichiometric calculations to estimate the amounts and assume 10% losses.

Table S18. Process inputs and outputs for preparation of zinc 2,4 pentadionate.

Input	Flow type	Quantity	Data source
Vinyl acetate	Eco	0.22 kg	
Zinc chloride	Eco	0.15 kg	
<b>Output</b>	<b>Flow type</b>	<b>Quantity</b>	<b>Data source</b>
Zinc 2,4 pentanedione	Eco	0.34 kg	

Table S19. Process inputs and outputs for synthesis of zinc chloride.

Input	Flow type	Quantity	Data source
Hydrochloric acid	Eco	0.08	
Zinc	Eco	0.07	
Output	Flow type	Quantity	Data source
Zinc chloride	Eco	0.14	

## 2.17. Lift-off

### 2.17.1. Laser lift-off

For lift-off practiced on a 10x10mm sample, the total energy consumption of the laser equipment was measured at 0.002 kWh (we disregard power consumption during startup and shutdown, assuming a large number of cells can be processed continuously). To this, we add 0.04 kWh for the ventilation equipment, which must operate after processing on the GaAs sample for safety reasons. The laser stage has an area of 762 x 432 mm, so we assume that 70 x 40 samples can be ventilated at a given time. Extrapolating this linearly to a cell (area 78.3 cm<sup>2</sup>), we get a total of:

$$\left( \frac{0.002 \text{ kWh}}{10 \times 10 \text{ mm}^2} + \frac{0.04 \text{ kWh}}{70 \times 40 \times 10 \times 10 \text{ mm}^2} \right) \cdot \frac{100 \text{ mm}^2}{\text{cm}^2} \cdot \frac{78.3 \text{ cm}^2}{\text{cell}} = \frac{0.16 \text{ kWh}}{\text{cell}}$$

### 2.17.2. Chemical lift-off

To compare the laser lift-off with a chemical method, we modelled a wet chemical process used to etch the bonding layer. Based on projections for state of the arte wet-chemical etching system, we assumed a consumption of 1,25 ml of 50% HF etching solution per wafer. The recyclability of the etching solution is very high, therefore we disregarded the wastewater treatment from this process.

## 2.18. GaAs substrate reuse and reclaim

We assumed that the GaAs substrate can be reused 100 times. However, this requires periodical chemical-mechanical polishing (CMP) of the GaAs substrate<sup>18</sup> which is done every 5 reuse cycles. We assume 98% process losses.

Table S20. Process inputs and outputs for reclaiming of GaAs substrate

Input	Flow type	Quantity	Data source
CMP slurry	Eco	0.2 L	Matovu et al. <sup>18</sup>
electricity	Eco	2 kWh	
Output	Flow type	Quantity	Data source
Reclaim of 1 GaAs substrate	Eco	1 unit	

Table S4. Energy and material inputs and outputs for CMP slurry

Input	Flow type	Quantity	Data source
Activated silica	Eco	100 g	Matovu et al. <sup>18</sup>
Hydrogen peroxide	Eco	33.33 g	Matovu et al. <sup>18</sup>
Water, deionised		866.67 g	Matovu et al. <sup>18</sup>
Output	Flow type	Quantity	Data source
CMP slurry	Eco	1 L	

### 2.19. III-V/Si PV electricity generation

The III-V/Si cells can be a drop-in replacement for commercially available single-Si PV systems. To make all infrastructure and BOS components equal in the III-V/Si and single-Si systems, we duplicated the ecoinvent (v3.4) process for generation of 1 kWh from a roof-mounted installation. We then replaced the single-Si cell for the III-V cell in the panel which was supplied to the installation, using the same cell area. The area of cell required to generate a given amount of electricity is inversely proportional to the conversion efficiency of the cell, so we applied the increased efficiency factor to the electricity output of the III-V/Si plant. The efficiency of the single-Si module in ecoinvent is 13.6%, and for the III-V/Si module is 28%, giving a conversion factor of  $(0.28/0.136) = 2.05$ . We applied this directly to the output of the III-V/Si installation, where instead of generating 1kWh it would generate 2.05 kWh with the same ancillary infrastructure and BOS components. The quantity of inverters required is proportional to power, not to area so we kept this constant for an output of 1kWh.

### 3. Sensitivity analysis of technological improvements

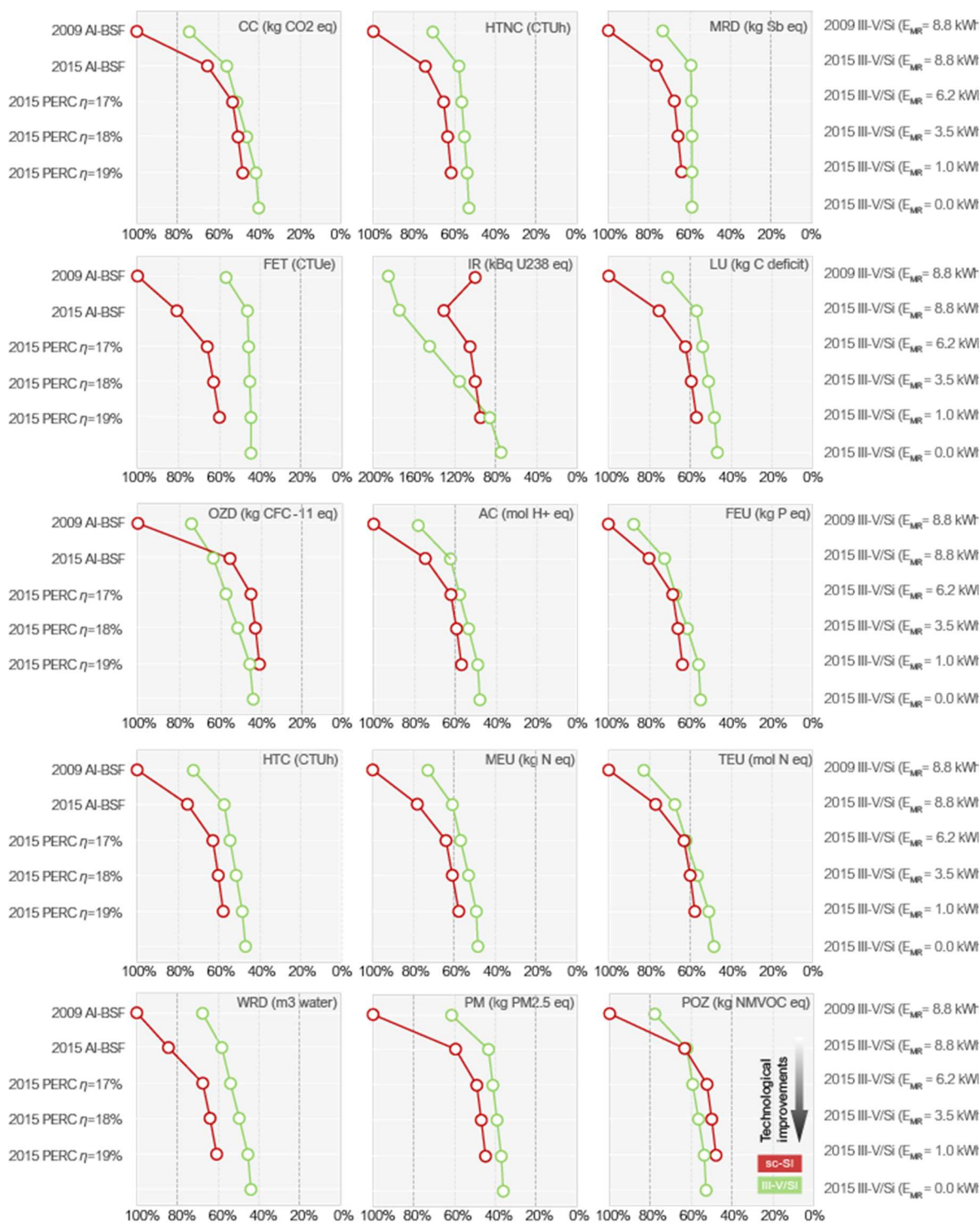


Figure S3. Change in impact scores as a result of technological improvements. 2009: Reference data (2009) for silicon, module and BOS supply chains from ecoinvent v3.4; 2015: Updated IEA PVPS data (2015) for silicon, module and BOS supply chains;  $\eta$ : module efficiency;  $E_{MR}$ : Energy consumption for a single MOVPE run of 37 wafers (2905 cm<sup>2</sup>).

## References

1. Louwen, A., Van Sark, W. G. J. H. M., Schropp, R. E. I., Turkenburg, W. C. & Faaij, A. P. C. Life-cycle greenhouse gas emissions and energy payback time of current and prospective silicon heterojunction solar cell designs. *Progress in Photovoltaics: Research and Applications* **23**, 1406–1428 (2015).
2. Paschotta, R. Wall-plug efficiency. *RP Photonics Encyclopedia* (2019).
3. Wood, D. *et al.* Passivated Busbars from Screen-printed Low-temperature Copper Paste. *Energy Procedia* **55**, 724–732 (2014).
4. Wernet, G. *et al.* The ecoinvent database version 3 (part I): overview and methodology. *Int. J. Life Cycle Assess.* **21**, 1218–1230 (2016).
5. Spath, P. L. & Mann, M. K. *Life cycle assessment of hydrogen production via natural gas steam reforming*. National Renewable Energy Laboratory (2001).
6. Mehmeti, A., Angelis-Dimakis, A., Arampatzis, G., McPhail, S. & Ulgiati, S. Life Cycle Assessment and Water Footprint of Hydrogen Production Methods: From Conventional to Emerging Technologies. *Environments* **5**, 24 (2018).
7. Cetinkaya, E., Dincer, I. & Naterer, G. F. Life cycle assessment of various hydrogen production methods. *Int. J. Hydrogen Energy* **37**, 2071–2080 (2012).
8. Balaji, R. *et al.* Development and performance evaluation of Proton Exchange Membrane (PEM) based hydrogen generator for portable applications. *Int. J. Hydrogen Energy* **36**, 1399–1403 (2011).
9. Smith, B. L., Babbitt, C. W., Horowitz, K., Gaustad, G. & Hubbard, S. M. Life Cycle Assessment of III-V Precursors for Photovoltaic and Semiconductor Applications. *MRS Adv.* **3**, 1399–1404 (2018).
10. Guerin, J. An increased portfolio for waste gas abatement. *Compound Semiconductors* 18–22 (2016).
11. Hsu, J.-N., Tsai, C.-J., Chiang, C. & Li, S.-N. Silane Removal at Ambient Temperature by Using Alumina-Supported Metal Oxide Adsorbents. *J. Air Waste Manage. Assoc.* **57**, 204–210 (2007).
12. Pacaud, B., Popa, J.-M. & Cartier, C.-B. Purification of silane gas. (1990).
13. CS Clean Systems. Safety Data Sheet - Cleansorb CS3C. (2014).
14. Wang, X. *et al.* Arsine adsorption in copper-exchanged zeolite under low temperature and micro-oxygen conditions. *RSC Adv.* **7**, 56638–56647 (2017).
15. Li, W.-C. *et al.* Metal Loaded Zeolite Adsorbents for Phosphine Removal. *Ind. Eng. Chem. Res.* **47**, 1501–1505 (2008).
16. Heitmann, U. *et al.* Novel Approach for the Bonding of III-V on Silicon Tandem Solar Cells with a Transparent Conductive Adhesive. in *2018 IEEE 7th World Conference on Photovoltaic Energy Conversion, WCPEC 2018 - A Joint Conference of 45th IEEE PVSC, 28th PVSEC and 34th EU PVSEC* 201–205 (IEEE, 2018). doi:10.1109/PVSC.2018.8548276
17. Chaudhuri, M. K. *et al.* Process for making metal acetylacetonates. (2002).
18. Matovu, J. B., Ong, P., Leunissen, L. H. A., Krishnan, S. & Babu, S. V. Fundamental Investigation

of Chemical Mechanical Polishing of GaAs in Silica Dispersions: Material Removal and Arsenic Trihydride Formation Pathways. *ECS J. Solid State Sci. Technol.* **2**, P432–P439 (2013).